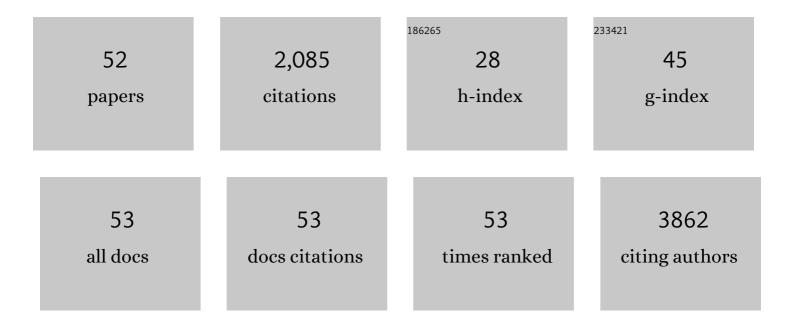
## **Xuefeng Song**

List of Publications by Year in descending order

Source: https://exaly.com/author-pdf/9216961/publications.pdf Version: 2024-02-01



#	Article	IF	CITATIONS
1	Selfâ€Assembled αâ€Fe <sub>2</sub> O <sub>3</sub> Mesocrystals/Graphene Nanohybrid for Enhanced Electrochemical Capacitors. Small, 2014, 10, 2270-2279.	10.0	177
2	Facile Synthesis of Nitrogen-Doped Graphene–Ultrathin MnO <sub>2</sub> Sheet Composites and Their Electrochemical Performances. ACS Applied Materials & Interfaces, 2013, 5, 3317-3322.	8.0	173
3	Covalently Coupled Ultrafine H-TiO <sub>2</sub> Nanocrystals/Nitrogen-Doped Graphene Hybrid Materials for High-Performance Supercapacitor. ACS Applied Materials & Interfaces, 2015, 7, 17884-17892.	8.0	119
4	Heating-Rate-Induced Porous α-Fe <sub>2</sub> O <sub>3</sub> with Controllable Pore Size and Crystallinity Grown on Graphene for Supercapacitors. ACS Applied Materials & Interfaces, 2015, 7, 75-79.	8.0	100
5	Active Fe <sub>2</sub> O <sub>3</sub> nanoparticles encapsulated in porous g-C <sub>3</sub> N <sub>4</sub> /graphene sandwich-type nanosheets as a superior anode for high-performance lithium-ion batteries. Journal of Materials Chemistry A, 2016, 4, 10666-10672.	10.3	94
6	Phyllosilicate evolved hierarchical Ni- and Cu–Ni/SiO2 nanocomposites for methane dry reforming catalysis. Applied Catalysis A: General, 2015, 503, 94-102.	4.3	78
7	Crumpled nitrogen-doped graphene–ultrafine Mn3O4 nanohybrids and their application in supercapacitors. Journal of Materials Chemistry A, 2013, 1, 14162.	10.3	72
8	Surfactant-free hydrothermal synthesis of Cu <sub>2</sub> ZnSnS <sub>4</sub> (CZTS) nanocrystals with photocatalytic properties. RSC Advances, 2014, 4, 27805-27810.	3.6	72
9	Photoelectrochemical Hydrogen Production of TiO <sub>2</sub> Passivated Pt/Si-Nanowire Composite Photocathode. ACS Applied Materials & Interfaces, 2015, 7, 18560-18565.	8.0	65
10	High rate lithium-ion batteries from hybrid hollow spheres with a few-layered MoS <sub>2</sub> -entrapped carbon sheath synthesized by a space-confined reaction. Journal of Materials Chemistry A, 2016, 4, 10425-10434.	10.3	63
11	Cu–Ni@SiO2 alloy nanocomposites for methane dry reforming catalysis. RSC Advances, 2013, 3, 23976.	3.6	59
12	A novel sound-based belt condition monitoring method for robotic grinding using optimally pruned extreme learning machine. Journal of Materials Processing Technology, 2018, 260, 9-19.	6.3	55
13	Facile synthesis of hollow hierarchical Ni/γ-Al <sub>2</sub> O <sub>3</sub> nanocomposites for methane dry reforming catalysis. RSC Advances, 2014, 4, 51184-51193.	3.6	50
14	Micro―and Nanostructures of Photoelectrodes for Solarâ€Đriven Water Splitting. Advanced Materials, 2015, 27, 562-568.	21.0	50
15	Cu <sub>2</sub> ZnSnS <sub>4</sub> thin films: spin coating synthesis and photoelectrochemistry. RSC Advances, 2014, 4, 21318-21324.	3.6	49
16	A MnOOH/nitrogen-doped graphene hybrid nanowires sandwich film for flexible all-solid-state supercapacitors. Journal of Materials Chemistry A, 2015, 3, 6136-6145.	10.3	49
17	Highly Conductive Mo <sub>2</sub> C Nanofibers Encapsulated in Ultrathin MnO <sub>2</sub> Nanosheets as a Self-Supported Electrode for High-Performance Capacitive Energy Storage. ACS Applied Materials & Interfaces, 2016, 8, 32460-32467.	8.0	49
18	Hollow hierarchical Ni/MgO-SiO2 catalyst with high activity, thermal stability and coking resistance for catalytic dry reforming of methane. International Journal of Hydrogen Energy, 2018, 43, 11056-11068.	7.1	44

XUEFENG SONG

#	Article	IF	CITATIONS
19	A Silicon/Double-Shelled Carbon Yolk-Like Nanostructure as High-Performance Anode Materials for Lithium-Ion Battery. Journal of the Electrochemical Society, 2015, 162, A1530-A1536.	2.9	42
20	A comprehensive study on surface integrity of nickel-based superalloy Inconel 718 under robotic belt grinding. Materials and Manufacturing Processes, 2019, 34, 61-69.	4.7	35
21	Confinement Effect of Mesopores: In Situ Synthesis of Cationic Tungsten-Vacancies for a Highly Ordered Mesoporous Tungsten Phosphide Electrocatalyst. ACS Applied Materials & Interfaces, 2020, 12, 22741-22750.	8.0	34
22	Engineering the volumetric effect of Polypyrrole for auto-deformable supercapacitor. Chemical Engineering Journal, 2019, 374, 59-67.	12.7	33
23	Generation of Monolayer MoS <sub>2</sub> with 1T Phase by Spatialâ€Confinementâ€Induced Ultrathin PPy Anchoring for Highâ€Performance Supercapacitor. Advanced Materials Interfaces, 2019, 6, 1900162.	3.7	33
24	Metal organic framework derived Ni/CeO2 catalyst with highly dispersed ultra-fine Ni nanoparticles: Impregnation synthesis and the application in CO2 methanation. Ceramics International, 2021, 47, 12366-12374.	4.8	33
25	Controlled synthesis of yolk–mesoporous shell Si@SiO <sub>2</sub> nanohybrid designed for high performance Li ion battery. RSC Advances, 2014, 4, 20814-20820.	3.6	32
26	Template-assisted synthesis of multi-shelled carbon hollow spheres with an ultralarge pore volume as anode materials in Li-ion batteries. RSC Advances, 2015, 5, 3657-3664.	3.6	32
27	Size-engineerable NiS 2 hollow spheres photo co-catalysts from supermolecular precursor for H 2 production from water splitting. Chemical Engineering Journal, 2016, 290, 74-81.	12.7	31
28	Recoverable Wire-Shaped Supercapacitors with Ultrahigh Volumetric Energy Density for Multifunctional Portable and Wearable Electronics. ACS Applied Materials & Interfaces, 2017, 9, 17051-17059.	8.0	31
29	Highly coke resistant Mg–Ni/Al <sub>2</sub> O <sub>3</sub> catalyst prepared <i>via</i> a novel magnesiothermic reduction for methane reforming catalysis with CO <sub>2</sub> : the unique role of Al–Ni intermetallics. Nanoscale, 2019, 11, 1262-1272.	5.6	29
30	Sol–gel nanocasting synthesis of kesterite Cu <sub>2</sub> ZnSnS <sub>4</sub> nanorods. RSC Advances, 2015, 5, 1220-1226.	3.6	28
31	Interfacial electrochemical investigation of 3D space-confined MnFe2O4 for high-performance ionic liquid-based supercapacitors. Electrochimica Acta, 2020, 331, 135386.	5.2	22
32	Ultrathin Ti-doped hematite photoanode byÂpyrolysis of ferrocene. International Journal of Hydrogen Energy, 2014, 39, 14596-14603.	7.1	21
33	Electrode material of core-shell hybrid MoS2@C/CNTs with carbon intercalated few-layer MoS2 nanosheets. Materials Today Energy, 2020, 16, 100379.	4.7	21
34	Engineering defectâ€enabled 3D porous MoS <sub>2</sub> /C architectures for high performance lithiumâ€ion batteries. Journal of the American Ceramic Society, 2020, 103, 4453-4462.	3.8	20
35	A robust quasiâ€superhydrophobic ceria coating prepared using airâ€plasma spraying. Journal of the American Ceramic Society, 2019, 102, 1386-1393.	3.8	19
36	Bioinspired pomegranate-like microflowers confining core-shell binary Ni <sub>x</sub> S <sub>y</sub> nanobeads for efficient supercapacitors exhibiting a durable lifespan exceeding 100 000 cycles. Journal of Materials Chemistry A, 2019, 7, 3432-3442.	10.3	19

XUEFENG SONG

#	Article	IF	CITATIONS
37	A robust hierarchical microcapsule for efficient supercapacitors exhibiting an ultrahigh current density of 300 A g <sup>â''1</sup> . Journal of Materials Chemistry A, 2018, 6, 5724-5732.	10.3	15
38	An Investigation of Surface Corrosion Behavior of Inconel 718 after Robotic Belt Grinding. Materials, 2018, 11, 2440.	2.9	14
39	A hierarchical hybrid design for high performance tin based Li-ion battery anodes. Nanotechnology, 2013, 24, 205401.	2.6	13
40	Visible Light-Activated Self-Recovery Hydrophobic CeO <sub>2</sub> /Black TiO <sub>2</sub> Coating Prepared Using Air Plasma Spraying. ACS Applied Materials & Interfaces, 2019, 11, 37209-37215.	8.0	13
41	Enhanced photoelectrochemical performance and stability of Si nanowire photocathode with deposition of hematite and carbon. Applied Surface Science, 2019, 471, 528-536.	6.1	13
42	Visible lightâ€activated degradation of microcystin‣R by ultrathin gâ€C <sub>3</sub> N <sub>4</sub> nanosheetsâ€based heterojunction photocatalyst. Journal of the American Ceramic Society, 2020, 103, 1281-1292.	3.8	13
43	Enhanced photoelectrochemical performance of planar p-Silicon by APCVD deposition of surface mesoporous hematite coating. Applied Catalysis B: Environmental, 2017, 200, 372-377.	20.2	12
44	Interface guide: In-situ integrating MoS2 nanosheets into highly ordered polypyrrole film for high performance flexible supercapacitor electrodes. Composites Science and Technology, 2020, 197, 108263.	7.8	12
45	Integrated Sustainable Wind Power Harvesting and Ultrahigh Energy Density Wireâ€Shaped Supercapacitors Based on Vertically Oriented Nanosheetâ€Arrayâ€Coated Carbon Fibers. Advanced Sustainable Systems, 2017, 1, 1700044.	5.3	11
46	Coating of Phosphide Catalysts on p-Silicon by a Necking Strategy for Improved Photoelectrochemical Characteristics in Alkaline Media. ACS Applied Materials & Interfaces, 2021, 13, 20185-20193.	8.0	10
47	Sustainable Energy System Utilizing Highâ€Voltageâ€Stable and Energyâ€dense Supercapacitors Based on Porous Fe <sub>2</sub> O <sub>3</sub> @Graphene Electrode in Ionic Liquid Electrolyte. Energy Technology, 2018, 6, 2399-2407.	3.8	7
48	Foamy Photocathode with Cu <sub>2</sub> O Nanowire Arrays Decorated with Cu <sub>2</sub> O and Carbon Layer for Photoelectrochemical Hydrogen Evolution. Journal of the Electrochemical Society, 2019, 166, H452-H458.	2.9	5
49	Self‣upporting Electrode of High Conductive PEDOT:PSS/CNTs Coaxial Nanocables Wrapped by MnO <sub>2</sub> Nanosheets. ChemistrySelect, 2019, 4, 2009-2017.	1.5	4
50	Enhancing the Long-Term Photoelectrochemical Performance of TiO <sub>2</sub> /Si Photocathodes by Coating of Ti-Doped Mesoporous Hematite. ACS Applied Energy Materials, 2021, 4, 7882-7890.	5.1	4
51	Hybrid Nanostructured Ni(OH)2/NiO for High-Capacity Lithium-Ion Battery Anodes. Journal of Electrochemical Energy Conversion and Storage, 2020, 17, .	2.1	4
52	Capacitors: Selfâ€Assembled αâ€Fe <sub>2</sub> O <sub>3</sub> Mesocrystals/Graphene Nanohybrid for Enhanced Electrochemical Capacitors (Small 11/2014). Small, 2014, 10, 2308-2308.	10.0	1